



Contents lists available at ScienceDirect

## Journal of Archaeological Science

journal homepage: <http://www.elsevier.com/locate/jas>

# A new local scale prediction model of Amazonian landscape domestication sites

Jungyu Choi<sup>a,\*</sup>, David K. Wright<sup>b</sup>, Helena Pinto Lima<sup>c</sup>

<sup>a</sup> Gyeongju National Research Institute of Cultural Heritage, Curatorial Affairs Division, Gyocheonan-gil 38, 38170, Gyeongju, Gyeongbuk, Republic of Korea

<sup>b</sup> University of Oslo, Department of Archaeology, Conservation and History, Blindernveien 11, 0371, Oslo, Norway

<sup>c</sup> Museu Paraense Emílio Goeldi, Coordenação de Ciências Humanas, Av. Perimetral, 1901 Terra Firme, Belém Pará, 66040-170, Brazil

## ARTICLE INFO

## Keywords:

Domesticated landscapes  
Amazonian Dark Earths  
Enhanced Vegetation Index  
Geographical Information Systems  
Getis-Ord's  $G_i^*$   
Anselin's Local Moran's  $I$

## ABSTRACT

Amazonia has drawn the interest of researchers over the last few decades as a region with evidence for extensive ancient/past indigenous landscape domestication. Among the major issues surrounding the nature of landscape domestication of pre-Columbian Amazonians, its scale is critically connected with other major problems in the history of Amazonia such as forms of urbanism, land engineering and agriculture. In recent years, some research in historical ecology has focused on developing methods to calibrate landscape domestication by interpreting the effects of human activity on the formation of the modern Amazonian landscape. This paper presents regional-scale research in the *Floresta Nacional de Caxiuanã* (FNC) to provide a method to trace and calibrate long-term forest management. With the data collected from the FNC and satellite images, the relationship between soils, an Enhanced Vegetation Index (EVI) and landscape domestication are explored. The data are interpreted as indicating that zones of anthropogenic enrichment of the soil due to forest management over the last 2000 years have a positive correlation with high EVI values. The research methods have potential to be applied broadly in tropical rainforest environments where pedestrian survey is difficult to undertake.

## 1. Introduction

The understanding of the cultural and natural complexion of Amazonia, from the arrival of humans in the region until the European colonization in the Americas after AD 1492, has significantly changed since the late 1990s with the introduction of historical ecology (Clement et al., 2015; Erickson, 2008). The traditional view on the prehistory of Amazonia can be summarized with the term 'Counterfeit Paradise' (Meggers, 1971), which was introduced by archaeologists during the 1960s and 1970s. The Counterfeit Paradise paradigm asserted that Amazonian cultures were in a state of decline, arriving at the peak of their cultural development during the late pre-colonial period and then declining due to the harsh environment of Amazonia with nutrient-poor soils and the lack of large game animals (Evans and Meggers, 1950; Meggers, 1971).

However, as Amazonian archaeology advanced, new discoveries were made, which provided evidence against the notion of a counterfeit paradise. Based on this new evidence, a revised view on the cultural history of Amazonia was introduced by historical ecologists based on

accumulating long-view data sets. One of the major advances in Amazonian archaeology was the scientific discovery and characterization of Amazonian Dark Earth (ADE) (Smith, 1980; Sombroek, 1966). ADE is an anthropogenic nutrient-rich dark-colored soil, also known as *Terra preta do Índio* or Amazonian Black Earth, which demonstrated that pre-Columbian Amazonian cultures were not culturally declining, but actually were actively managing and altering the environment for many hundreds of years. Historical ecologists have termed this process 'landscape domestication' (Balée, 1998; Balée and Clark, 2006; Clement et al., 2015; Erickson, 2008), which implies that there are fuzzy boundaries on quantifiable human impacts due to the difficulties of tracing landscape-scale activities. Nevertheless, since its introduction, the extent and nature of landscape domestication has become one of the most important research foci in Amazonian archaeology (Clement et al., 2015).

There are several research topics that are subjected to the research of the landscape domestication in Amazonia, including the domestication of plant species (Levis et al., 2017; Lins et al., 2015), forest management activities (Junqueira et al., 2011), and formation of ADE (Hecht, 2003;

\* Corresponding author.

E-mail addresses: [jungyu.choi90@gmail.com](mailto:jungyu.choi90@gmail.com), [unterboot571@korea.kr](mailto:unterboot571@korea.kr) (J. Choi), [david.wright@iakh.uio.no](mailto:david.wright@iakh.uio.no) (D.K. Wright), [helenalima@museu-goeldi.br](mailto:helenalima@museu-goeldi.br) (H.P. Lima).

<https://doi.org/10.1016/j.jas.2020.105240>

Received 25 February 2020; Received in revised form 25 August 2020; Accepted 27 August 2020

Available online 18 September 2020

0305-4403/© 2020 Elsevier Ltd. All rights reserved.



Fig. 1. The map of Amazonia and the location of the FNC.

Winklerprins, 2009; Schmidt et al., 2014). One of the major research directions of the landscape domestication of Amazonia is understanding its scale. Combined with the problem of gauging the population levels of pre-Columbian Amazonians, the scale of the impact that Amazonians made on the landscape is one of the most actively debated subjects related to landscape domestication in Amazonia (Bush and Silman, 2007; Bush et al., 2008; Clement et al., 2015; McMichael et al., 2012; McMichael et al., 2014). Attempts made to determine the scale of landscape domestication mainly focused on the attempt to identify the extent of ADE distribution in Amazonia (McMichael et al., 2014; Palace et al., 2017; Thayn et al., 2011), but due to the vast extent of Amazonia and the insufficient accumulation of survey data from across the entire region caused by the difficulty of surveys performed in the tropical rainforest, the debate goes on (Santos et al., 2018).

In addition, statistical methods that applied remote sensing tools were introduced as ways to define the extent of anthropogenesis of Amazonia (for a recent review, see Santos et al., 2018). These methods utilize data obtained from satellite images to directly interpret pre-Columbian landscape domestication based on the vegetation patterns found across the modern landscape. However, to trace and calibrate the landscape domestication activities of the past by interpreting the modern landscape, further understanding of the relationship between the pre-Columbian landscape domestication and the modern landscape of Amazonia is required.

Here, we present a predictive model of the location of pre-Columbian landscape domestication sites, using the public domain Advanced Spaceborne Thermal Emission and Reflection Radiometer (ASTER) L1T satellite images in combination with spatial autocorrelations generated using Geographic Information Systems (GIS). We utilize the Enhanced Vegetation Index (EVI) as an indicator to identify areas affected by pre-

Columbian landscape domestication activities. Researchers who utilize remote sensing as a research tool started to focus on Vegetation Indices (VIs) as a device that can be used in Amazonian archaeology, mostly to locate or predict ADE sites (Palace et al., 2017; Russell, 2005; Thayn et al., 2009; Thayn et al., 2011), since it has been demonstrated that soils are affected by landscape domestication activities in various ways (Arroyo-Kalin, 2014; Arroyo-Kalin et al., 2009; Birk et al., 2011; Browne Ribeiro, 2014; Costa et al., 2013; Fraser et al., 2011; Lehmann et al., 2003; Levis et al., 2018; Macedo et al., 2017; Pinter et al., 2011; Schmidt et al., 2014; Winklerprins, 2009). Our methods first test whether the difference of soil types can be detected by EVI values through one-way analyses of variance (ANOVA). Then a prediction model using the EVI, and Getis-Ord's  $G_i^*$  and Anselin's Local Moran's  $I$  spatial autocorrelations is tested on whether areas affected by landscape domestication and areas that are less affected by landscape domestication can be spatially discriminated. Finally, a field study conducted in the Caxiuanã National Forest (*Floresta Nacional de Caxiuanã*, FNC) documents the varying physical characteristics of areas affected by landscape domestication activities identified in the geospatial model and postulates the effect they have on vegetation. Ultimately, this spatial model effectively identifies hotspots of anthropic activity, both past and present.

## 2. Materials and methods

### 2.1. Study area

The FNC is located in the municipalities of Portel and Melgaço, state of Pará, Brazil, and it covers an area of approximately 330,000 ha between the lower Xingu and the Tocantins rivers in the lower Amazon region approximately 350 km west of the city of Belém. The study area is

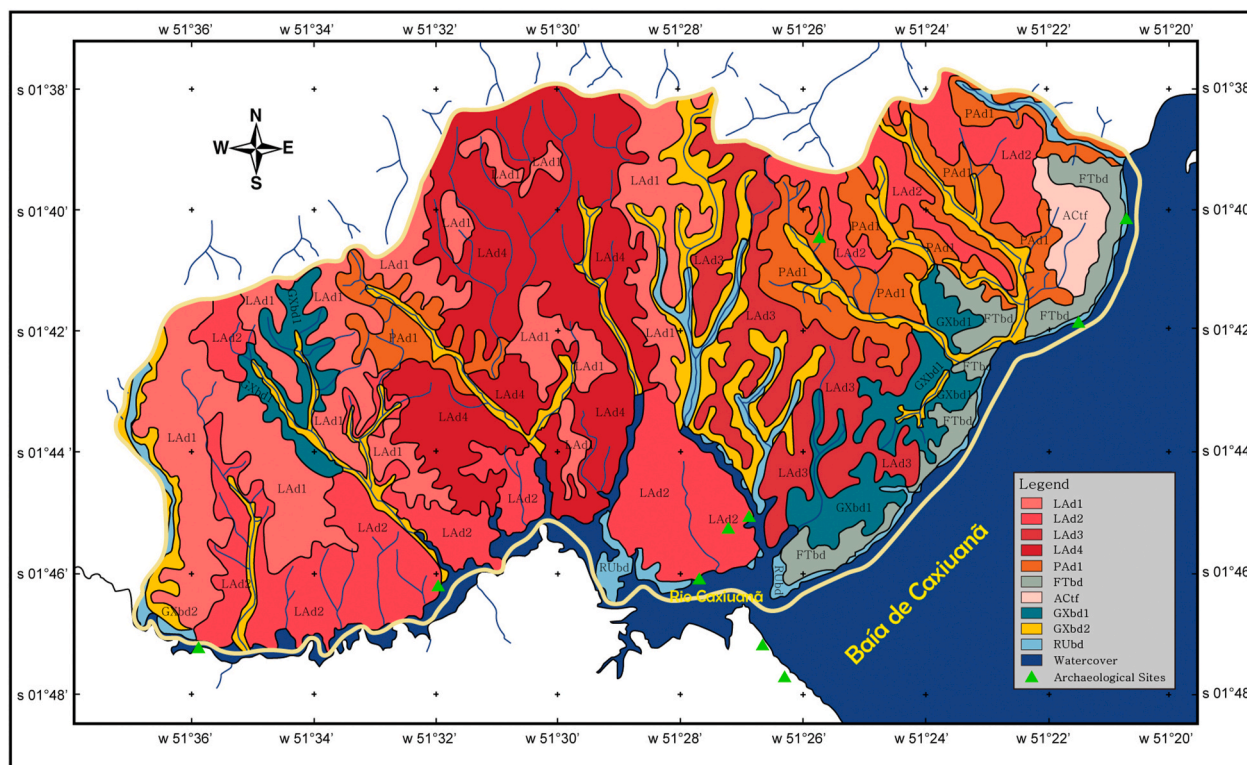


Fig. 2. Soil map of northern Caxiuana (Costa et al., 2005). Digitized with the permission of the MPEG. The area covered is indicated as 'Soil Survey Area' in Fig. 1.

limited to the border of the FNC for two major reasons. One is that the FNC is a conservation unit managed by the Brazilian government, which has limited the effects of modern human activities on the landscape to relatively controlled areas compared to other regions. This factor makes the FNC as an attractive place to conduct research on the relationship between the pre-Columbian landscape domestication and the modern environment. Another important reason is that detailed research on the environment of the FNC has been made due to the establishment of the Ferreira Penna Scientific Station (*Estação Científica Ferreira Penna*, ECFPn) by the Emílio Goeldi Museum of Pará (*Museu Paraense Emílio Goeldi*, MPEG) (Lisboa et al., 2013) since 1990. The environmental research includes a detailed soil survey of the area near the ECFPn (Fig. 2) (Costa et al., 2005), which is not widely available in other regions. The mapped soil contains significant potential to explore the relationship between soil and landscape domestication activities.

Human occupations were present in the FNC no later than  $2150 \pm 75$  BP according to the thermoluminescence dating of the pottery found in the area (Behling and da Costa, 2000; Coirolo and d'Aquino, 2005). By 2005, 32 archaeological sites were identified throughout the FNC, with 29 of the sites inside the boundary of the FNC and three of them outside the border, through surveys and several excavations that have been carried out by MPEG (Coirolo and d'Aquino, 2005), and two sites have been identified since this study. The 29 sites inside the border of the FNC were utilized for the analyses in this research. The sites identified are generally located on the banks of Caxiuana Bay, rivers, or small streams flowing through the forest (*igarapés*), on higher ground than, rest of the landscape (Lisboa et al., 2013). Elevation relative to water sources is said to be an important factor for the settlement locations of prehistoric people since archaeological sites tend to be located on *terra firme* rather than the lower wetlands (Lisboa et al., 2013).

The overall pre-Columbian/pre-colonial population density in the FNC has been hypothesized to have been low, based on the relatively sparse amount of charcoal found in the core samples collected from the bottom of the Curuá River (Behling and da Costa, 2000). However, excavations of archaeological sites, such as Ilha de Terra, identified

extensive deposits of ADE associated with dense layers of cultural debris, with more than 1300 fragments in five excavation units (Costa, 2003; Kern, 2004). ADE was identified in more than 90% of the sites identified in the FNC (Lisboa et al., 2013). Also, excavation which took place in 2016, near the research station of the Brazilian Institute of Environment and Renewable Natural Resources (*Instituto Brasileiro do Meio Ambiente e dos Recursos Naturais Renováveis*, IBAMA) has also identified the deep layer of ADE along with an intense concentration of archaeological materials, mainly consisting of pottery, shells and organic refuse (mainly animal bones and carbonized seeds). Since ADE associated with the intense deposits of cultural debris is commonly interpreted as a proxy for intensive human habitation (Clement et al., 2015; Smith, 1980), there is a strong possibility of a revised pre-colonial population estimate in the FNC in the future.

## 2.2. Satellite imagery and EVI

Vis are spectral transformations of two or more bands, which are structured to enable the comparisons of terrestrial photosynthetic activity and canopy structural variations spatially and temporally (Huete et al., 2002). Therefore, Vis can be used to monitor seasonal, inter-annual, and long-term variations of vegetal structure, phenological, and biophysical parameters (Huete et al., 2002), and to interpret characteristics of plans such as photosynthetic activity and plant productivity (Ma et al., 2001), and regional differences in the intensity of species composition of vegetation caused by anthropic effects (Walsh et al., 2001). Since ADE occurrence demonstrates chemical characteristics that affect the conditions of vegetation, such as available nutrient content with their adjacent soils (Lehmann et al., 2003), if the combination of vegetation species shows a certain degree of uniformity, the ADE will provide different VI values from non-ADE soils.

Among the Vis, Normalized Differential Vegetation Index (NDVI) is one of the most frequently employed VI. Field and laboratory research have demonstrated that NDVI has a strong correlation with fractions of active photoabsorbent vegetation and leaf area index (Palace et al.,

**Table 1**  
Description of soil types indicated in Fig. 2 (Costa et al., 2009). Soil classification according to Santos et al. (2006).

Code	Soil Class and Description	Area (ha)
	<i>YELLOW LATOSSOLO</i>	
LAd1	YELLOW LATOSSOLO: typical dystrophic; very clayey texture; moderate A horizon; subtropical forest; flat, smooth and wavy relief	6279
LAd2	YELLOW LATOSSOLO: typical dystrophic; medium texture; moderate A horizon; subtropical forest; flat, smooth and wavy relief	6761
LAd3	YELLOW LATOSSOLO: typical dystrophic; clayey texture; moderate A horizon; subtropical forest; flat, smooth and wavy relief	2745
LAd4	YELLOW LATOSSOLO: typical dystrophic; clayey texture; moderate A horizon; subtropical forest; flat, smooth and wavy relief + YELLOW LATOSSOLO: typical dystrophic; medium texture; moderate A horizon; subtropical forest; flat, smooth and wavy relief	5900
	<i>YELLOW ARGISSOLO</i>	
PAd1	YELLOW ARGISSOLO: typical dystrophic; medium/clayey texture; moderate A horizon; subtropical forest; flat, smooth and wavy relief + YELLOW LATOSSOLO: typical dystrophic; medium texture; moderate A horizon; subtropical forest; flat, smooth and wavy relief	3000
	<i>CLAY ILLUVIATED PLINTOSSOLO</i>	
FTbd	CLAY ILLUVIATED PLINTOSSOLO: typical dystrophic; medium/clayey texture; moderate A horizon; subtropical forest; flat, smooth and wavy relief + inclusion of CLAY ILLUVIATED PLINTOSSOLO: Ta Eutrophic anthropogenic; medium/clayey texture; anthropic A horizon; subtropical forest (of lowland)	1309
	<i>CHROMIC ALISSOLO</i>	
ACTf	CHROMIC ALISSOLO: Ta clay illuviated (clay with activity $^{320} \text{ cmol kg}^{-1}$ ) plinthic; medium/clayey texture; moderate A horizon; subtropical forest, flat, smooth and wavy relief	504
	<i>HAPLIC GLEISSOLO</i>	
GXbd1	HAPLIC GLEISSOLO: Ta dystrophic (clay with high activity and low base saturation (<50%) in most of the first 100 cm of the B or BA horizon) with aluminum character; silty texture; moderate A horizon; lowland equatorial forest; flat relief	2000
GXbd2	HAPLIC GLEISSOLO: Tb typical dystrophic (clay with low activity and low base saturation (<50%) in most of the first 100 cm of the B or BA horizon); silty texture; moderate A horizon; lowland equatorial forest; flat relief + FLUVIAL NEOSSOLO: Tb typical dystrophic; mixed texture; moderate A horizon; lowland equatorial forest; flat relief	3500
	<i>FLUVIC NEOSSOLO</i>	
RUbd	FLUVIC NEOSSOLO: Ta typical dystrophic (clay with high activity and low base saturation (<50%) in most of the first 100 cm of the B or BA horizon); mixed texture; moderate A horizon; lowland equatorial forest; flat relief + HAPLIC GLEISSOLO: Ta typical dystrophic; silty texture	1000
	Total	33,000

**Table 2**  
Summarized statistics of EVI distinguished by soil types. The description of the soil codes is presented in Table 1. Values smaller than 0.8753 were excluded from the analysis.

Soil Type	N	Mean	Std. Deviation	Std. Error	95% Confidence Interval for Mean		Minimum	Maximum
					Lower Bound	Upper Bound		
FTbd	17882	.9826	.0689	.0005	.9816	.9836	.8753	1.2352
GXbd1	33861	.9772	.0617	.0003	.9766	.9779	.8753	1.2500
GXbd2	37241	.9530	.0556	.0002	.9525	.9536	.8753	1.2678
LAd1	49438	.9412	.0462	.0002	.9408	.9416	.8753	1.1979
LAd2	160310	.9587	.0575	.0001	.9585	.9590	.8753	1.3121
LAd3	40304	.9910	.0608	.0003	.9904	.9916	.8753	1.2752
LAd4	79468	.9409	.0461	.0001	.9406	.9413	.8753	1.1813
PAd1	2063	.9421	.0476	.0010	.9400	.9441	.8753	1.1728
RUbd	16721	.9844	.0615	.0004	.9835	.9853	.8753	1.2752
Total (All Soil Types)	437288	.9593	.0579	.0000	.9591	.9595	.8753	1.3121

2017; Russell, 2005). Due to such a correlation, NDVI is widely used among various disciplines and regions (Borini Alves et al., 2015; Gandhi et al., 2015; Morton et al., 2006; Palace et al., 2017; Russell, 2005).

While NDVI is the most frequently used VI, it contains potential deficiencies caused by atmospheric effects and background brightness (Yamamoto et al., 2010). EVI was developed to overcome this limitation of NDVI. EVI is normally calculated by the following equation:

$$EVI = 2.5 * \frac{(NIR - Red)}{(NIR + 6 * Red - 7.5 * Blue + 1)}$$

EVI is more sensitive in regions with high biomass, reduces the atmospheric effect in satellite images, and as a result, provides an enhanced vegetation signal (Jiang et al., 2008; Yamamoto et al., 2010). Amazonia is an area with dense vegetation cover and a high moisture regime, which makes it appropriate to apply EVI for research (Jiang et al., 2008).

However, it has been pointed out by Thayn et al. (2009), that distinguishing ADEs from adjacent Oxisols or Ultisols is complicated by the differences which occur on the vegetation growing on the soils, which are more subtle than the differences between the soils themselves. Also, the results shown by Fraser et al. (2011) demonstrate that ADE are not subject to homogenous formation and taphonomic processes. There is presently no uniform method to discriminate ADEs from surrounding soils despite the known differences in soil nutrient availability between onsite and offsite contexts.

Even though there are difficulties present in distinguishing ADEs from non-ADE soils, it can be possible to identify the differences if the slight differences between EVI off- and on-site are systematically quantified and amplified. Although the differences may be subtle, it is clear that soils affected by anthropic activities demonstrate different characteristics with adjacent soils, and the differences become more evident moving towards the center of the core fertility of ADE sites (Fraser et al., 2011). Therefore, it can be said that although the difference in value may be minute along the perimeter of the features, the centers of ADE sites will, on average, provide more pixels with higher EVI values. In other words, it is possible to study the spatial autocorrelation of EVI values in order to map the distribution of ADE to trace landscape domestication activities.

In this research design, ASTER L1T images were used to create EVI values. Among the data provided by non-commercial satellite-based

**Table 3**  
Result of ANOVA on the effects of soil types to EVI.

	Sum of Squares	df	Mean Square	F	Sig.
Between Groups	116.711	8	14.589	4715.975	.000
Within Groups	1352.725	437279	.003		
Total	1469.436	437287			

**Table 4**  
Result of Scheffe's post-hoc test demonstrating homogeneous subsets.

Soil Class	N	Subset for alpha = 0.05					
		1	2	3	4	5	6
LAd4	79468	0.9409					
LAd1	49438	0.9412					
PAd1	2063	0.9412					
GXbd2	37241		0.9531				
LAd2	160310			0.9588			
GXbd1	33861				0.9773		
FTbd	17882					0.9826	
RUbd	16721					0.9845	
LAd3	40304						0.9910
Sig.		0.957	1.000	1.000	1.000	0.578	1.000

Means for groups in homogeneous subsets are displayed.

Uses Harmonic Mean Sample Size = 12487.804.

The group sizes are unequal. The harmonic mean of group sizes is used. Type I error levels are not guaranteed.

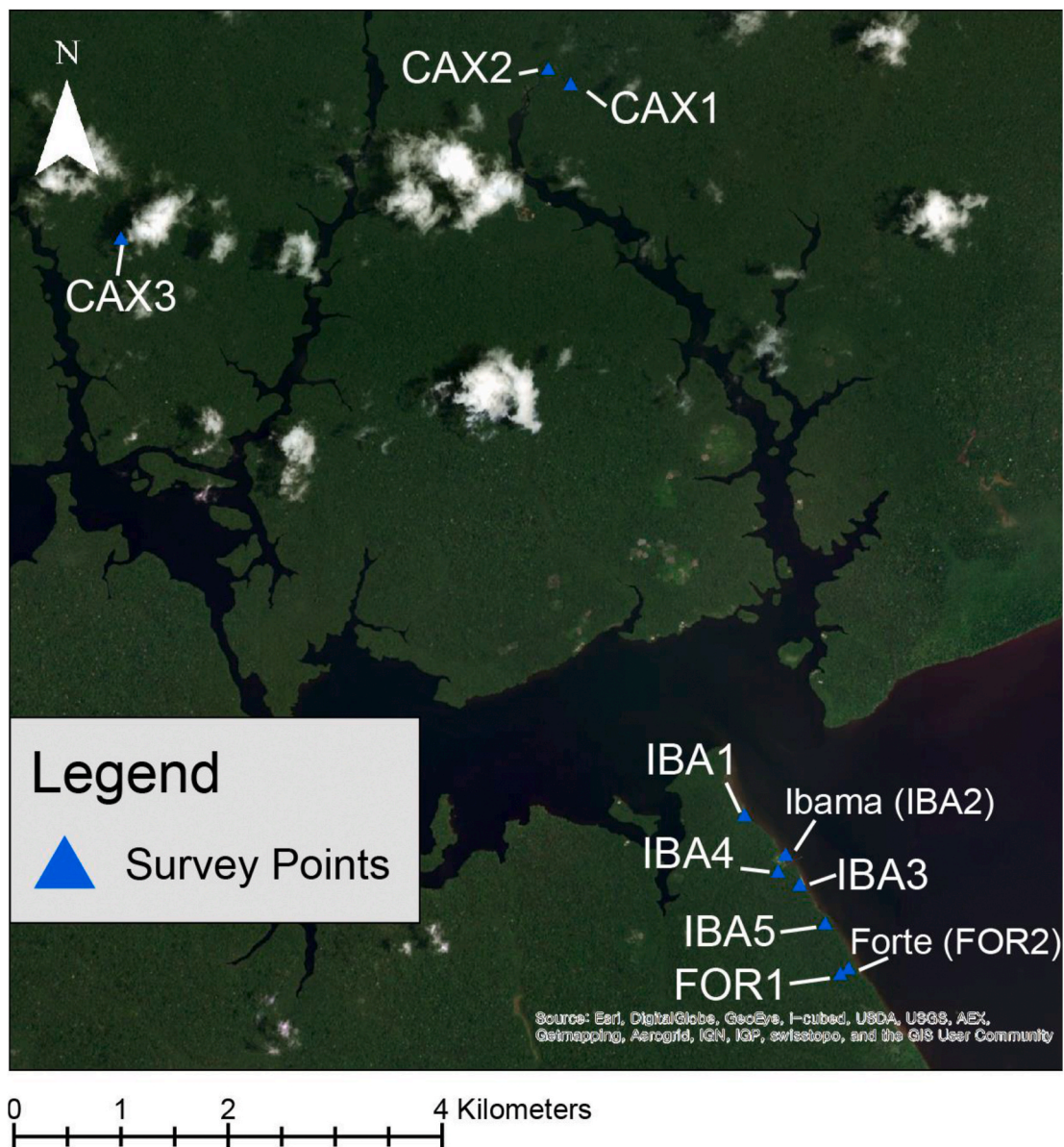


Fig. 3. Location of the points where pedestrian survey was undertaken.

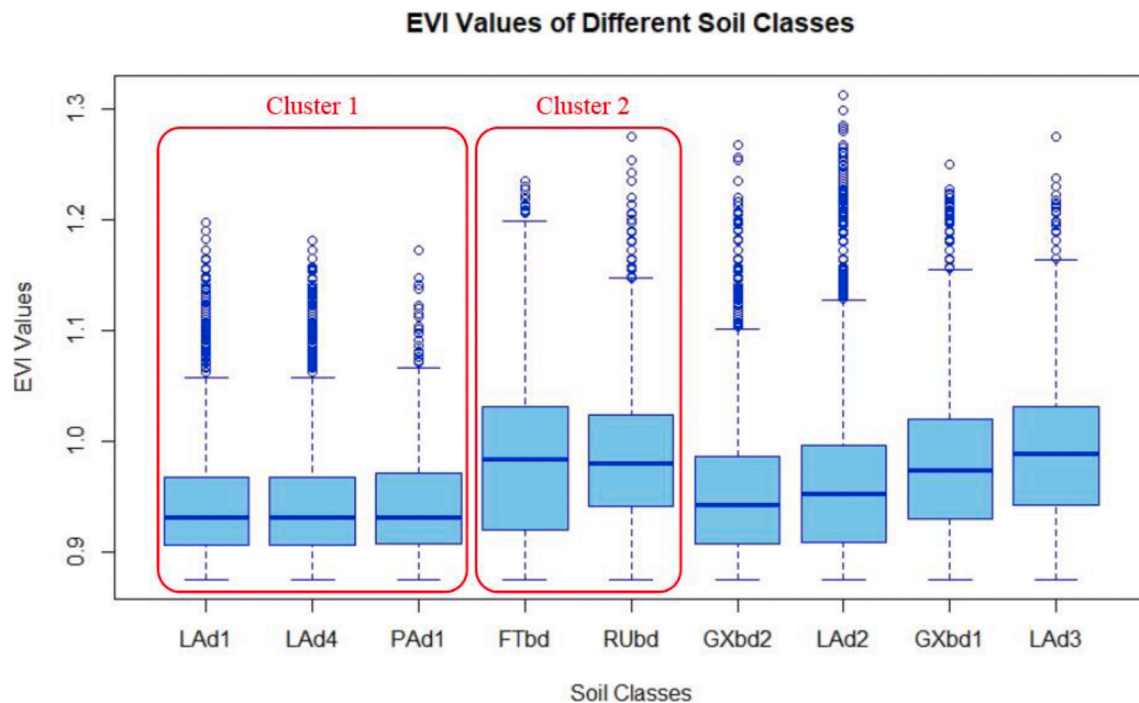


Fig. 4. Boxplot of EVI values according to soil classes. The clusters are grouped by the result of Scheffe’s post-hoc test.

sensors, the ASTER series products offer a spatial resolution of 15 m/pixel, which is relatively fine when compared to the spatial resolution of other products, such as the Landsat series (30 m/pixel) and Moderate Resolution Imaging Spectroradiometer (MODIS) series (250 m/pixel). Two satellite images of ASTER L1T dated to June 22, 2007 were downloaded from the United States Geological Survey’s (USGS) Earth Explorer website (<http://earthexplorer.usgs.gov/>). These images were selected for two reasons. First, the images contained the least amount of cloud cover relative to other images available in the data repository ( $\leq 2\%$ ), while covering most of the area of the FNC. Second, the variance between the VI values is the greatest between June and July in Amazonia throughout the year, with tropical rainforests demonstrating higher values than other types of land cover, such as pastures, agricultural fields, or savannah (Arvor et al., 2011).

The EVI was calculated using an alternate formula to the traditionally used one since ASTER does not collect blue frequency spectra (459–479 nm). There are currently three alternate formulas to calculate EVI by using only NIR and red frequencies (Yamamoto et al., 2010). However, one of these was developed for application in snow-covered areas, and therefore, it is not applicable in this research. One of the other two methods to calculate EVI involves reflectance values from ASTER and MODIS sensors (Yamamoto et al., 2010). This method, named as  $EVI_C$ , is possible since the ASTER and MODIS sensors are both loaded on the same Terra platform and there are possibilities of simultaneous observation of specific areas (Yamamoto et al., 2010). The formula involves NIR and red reflectance of the ASTER sensor, and blue reflectance of the MODIS sensor (Yamamoto et al., 2010). The other method, named as  $EVI_2$ , simply uses the NIR and visible red bands of ASTER (Jiang et al., 2008).

$EVI_C$  and  $EVI_2$  values were validated by comparison with EVI values calculated from MODIS data with the original formula. While  $EVI_2$  values showed a very close 1:1 correlation with the EVI data (Jiang et al., 2008),  $EVI_C$  showed lower correlation (0.960) than  $EVI_2$ , which seems to be a result of possible atmospheric effects in the MODIS blue reflectance values (Jiang et al., 2008; Yamamoto et al., 2010). Therefore, EVI was calculated using the  $EVI_2$  formula:

$$EVI_2 = 2.5 * \frac{\rho_{ASTER\ NIR} - \rho_{ASTER\ red}}{\rho_{ASTER\ NIR} + 2.4 * \rho_{ASTER\ red} + 1}$$

Before utilizing the calculated EVI for analyses, low EVI values, which are often caused by water, roads, and cloud cover, were excluded by statistically sorting out anomalous values. The mean value of EVI was 0.93 with a standard deviation of 0.06, so only EVI values greater than 0.87 were analyzed. The EVI values analyzed are from areas covered with forest vegetation excluding low or minimally vegetated regions from the analyses.

### 2.3. Evaluating the reflectance of soil types on EVI

Before testing the model to predict the areas affected by landscape domestication, it should be evaluated whether different soil properties actually do affect the expression of EVI within the study area. ANOVA test was executed using the soil survey result of Costa et al. (2005). The purpose of the ANOVA test was to demonstrate whether classifications of soil types are reflected in the EVI values. If the results demonstrate that the EVI values differ by soil types, it will provide the basis for locating spatially distinct areas for the application of spatial autocorrelation of EVI values. A post-hoc Scheffe test was subsequently performed after the ANOVA test to identify the differences in the mean EVI values between soil classes. These tests establish the framework for autocorrelation, which utilizes local (neighborhood) values to find outlying data clusters. If soil conditions do not affect vegetation growth/EVI values, the applicability of spatial autocorrelation using satellite imagery would be suspect, and the basis for proceeding with the analysis may not be justified.

To perform the ANOVA, the soil map (Fig. 2) presented in Costa et al. (2005) was integrated into a GIS by digitizing it into polygons with ArcGIS 10.2.2. Also, the EVI values were vectorized from a raster format using ‘Raster to Point’ tool. The information from the soil types was then spatially joined to points, which contain the EVI values in 15-m intervals. For ANOVA tests, the soil classes were set as independent variables, and EVI values were designated as dependent variables. The null hypothesis of the ANOVA test is that the population distribution of vegetation spectra is randomly distributed across the study area and that

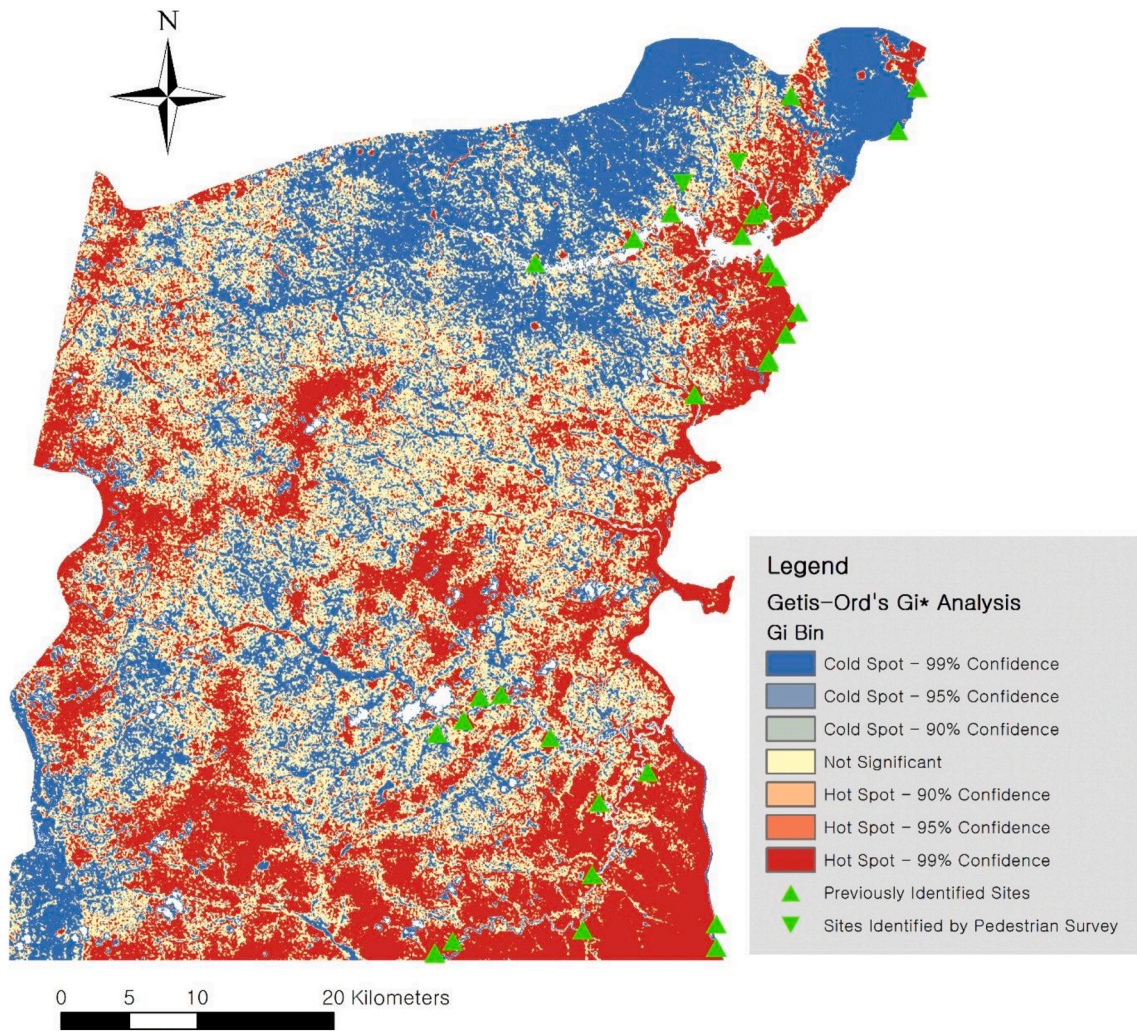


Fig. 5. The model created through Getis-Ord's Gi\* analysis of EVI values.

the variance of the values falls along a normal continuum (Pandit, 2010). If the F value, which indicates the influence of the effect, is significantly large and the significance of the results rejects the null hypothesis, it means that the conditions (in this case the soil class) (Pandit, 2010) non-randomly affect the distribution of vegetation spectra within different analytical zones with statistical significance determined by the p-value. The ANOVA/Scheffe's post-hoc test between the independent and dependent variables, soil class and EVI values, was analyzed using IBM SPSS 23.

2.4. Creating the predictive model for the areas affected by landscape domestication

After the effects of soils on EVI were investigated, the relationship between landscape domestication and EVI was examined through creating a predictive model for areas affected by landscape domestication. The models were created by applying spatial autocorrelation methods using ArcGIS 10.2.2. The first spatial autocorrelation method that applied was Getis-Ord's Gi\*. Getis-Ord's Gi\* is one variant in a family of spatial statistics called G, introduced by Getis and Ord (1992). Gi\* allows identification of local clustering patterns, which may not appear in global statistics, G (Ord and Getis, 1995). As a result, Gi\* can be applied more flexibly when compared to global statistics G, which cannot accommodate spatially variable clustering patterns. Getis-Ord's Gi\* index is defined by the following equation (Ord and Getis, 1995):

$$G_i^* = \frac{\sum_{j=1}^n w_{ij}x_j - \bar{X}\sum_{j=1}^n w_{ij}}{S\sqrt{\frac{[n\sum_{j=1}^n w_{ij}^2 - (\sum_{j=1}^n w_{ij})^2]}{n-1}}}$$

where

$$\bar{X} = \frac{\sum_{j=1}^n x_j}{n}$$

and

$$S = \sqrt{\frac{\sum_{j=1}^n s_j^2}{n} - (\bar{X})^2}$$

In this equation,  $x_j$  is the attribute value of feature  $j$ ,  $n$  is the total number of features,  $w_{ij}(d)$  is a binary spatial weighted matrix that defines  $w_{ij}$ . When locations of two features  $i$  and  $j$  are within the defined distance  $d$ ,  $w_{ij}$  is 1; otherwise,  $w_{ij}$  is 0. Calculated  $\bar{X}$  is the simple mean, and  $S$  is the simple variance (Ord and Getis, 1995).

The Gi\* value was compared with the z-score to examine whether clustering occurs (Getis and Ord, 1992). With a confidence level of 90%, the p-value, which indicates the probabilistic posterior distribution, should be smaller than 0.10. For the Gi\* to be statistically significant, it is conventionally understood that the value should be larger than 1.65 or smaller than -1.65, which are the corresponding z-scores to p-values (ESRI, 2016).

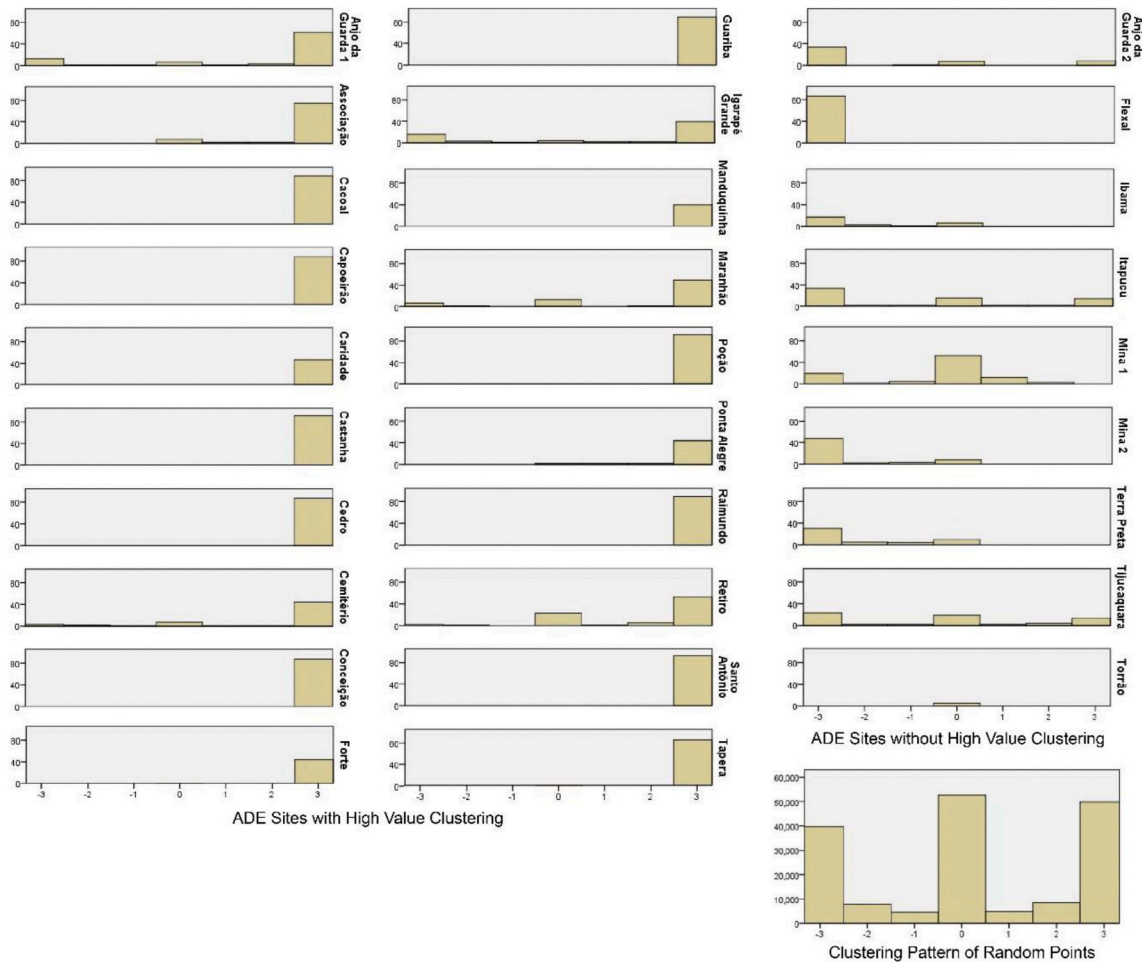


**Fig. 6.** The classification of the sites into ‘ADE sites with High-Value Clustering’ and ‘ADE Sites without High-Value Clustering’ according to the model created by Getis-Ord’s  $G_i^*$  analysis of EVI values. The numbers of the x-axis indicate the  $G_i\_Bin$  (−3 = Cold Spot - 99% Confidence, −2 = Cold Spot - 95% Confidence, −1 = Cold Spot - 90% Confidence, 0 = Not Significant, 1 = Hot Spot - 90% Confidence, 2 = Hot Spot - 95% Confidence, 3 = Hot Spot - 99% Confidence). The y-axis indicates the number of points. The classification was made by comparing the percentage of the points classified with the  $G_i\_Bin$  value 3. If the sites consisted of a higher percentage of points with the value of 3 than 2000 randomly generated points that represent the FNC, they were classified as ‘ADE Sites with High-Values Clustering.’ If not, they were classified as ‘ADE Sites without High-Value Clustering.’

Therefore, as a result of the Getis-Ord’s  $G_i^*$  analysis, each vectorized point of EVI was given a z-score, p-value, and confidence level bin ( $G_i\_Bin$ ). The  $G_i\_Bin$ , which is given as integer values between −3 and 3, is what indicates the statistically significant spatial clusters of high values (hotspots) and low values (coldspots). The degree of statistical significance is demonstrated through  $G_i\_Bin$  as well. Features with the  $G_i\_Bin$  value of ±3 are statistically significant at a 99 percent confidence level; those with ±2  $G_i\_Bin$  value are significant at the 95% confidence level; ±1  $G_i\_Bin$  indicates statistical significance at a 90% confidence level; 0 indicates that clustering for features is not statistically significant (ESRI, 2016).

The second method that was applied was Anselin’s Local Moran’s I. While Getis-Ord’s  $G_i^*$  clarifies areas characterized by very high values and very low values, Local Moran’s I focuses more on expressing the clustering of similar attribute values (Coluzzi et al., 2010). Local Moran’s I index is expressed by the following equation:

$$I_i = \frac{x_i - \bar{X}}{S_i^2} \sum_{j=1, j \neq i}^n w_{ij} (x_j - \bar{X})$$

In this equation,  $x_i$  is the attribute of,  $\bar{X}$  is the average of features, and  $w_{ij}$  is the spatial weight between feature  $i$  and feature  $j$  (Kim, 2012).

Anselin’s Local Moran’s I uses pseudo significance, which is expressed by pseudo p-values—a probabilistic statistic that examines the

significance of statistics (Anselin, 1995). The pseudo p-values are generated by comparing the actual Local Moran’s I value with the values produced by random permutations of points from spatially parameterized data (ESRI, 2016).

By executing Anselin’s Local Moran’s I analysis, z-score, pseudo p-value, and cluster/outlier type (C0type) is given to each of the EVI points. The cluster/outlier type is determined by the z-score and p-value. When the z-score is a high positive value, it indicates that the point has similar values with neighboring points, demonstrating a clustering pattern. When the z-score is a low negative value, the analyzed feature can be classified as an outlier from its surrounding features. Therefore, the C0Type classifies the points into five classes, which are high-value clusters (HH), low-value clusters (LL), high-value outliers surrounded by low values (HL), low value outliers surrounded by high values (LH), and features that do not demonstrate any statistical significance (Not Significant). The confidence level of the statistical significance of the results of Anselin’s Local Moran’s I is automatically fixed to 95% (ESRI, 2016).

A threshold distance needs to be set for Getis-Ord’s  $G_i^*$  and Anselin’s Moran’s I. A threshold distance indicates the range that features within it are acknowledged as neighboring to the target feature of analysis. For Getis-Ord’s  $G_i^*$ , the type of the threshold distance can be chosen between fixed distance band and inverse distance. While a default threshold distance can be computed, it is recommended to set a

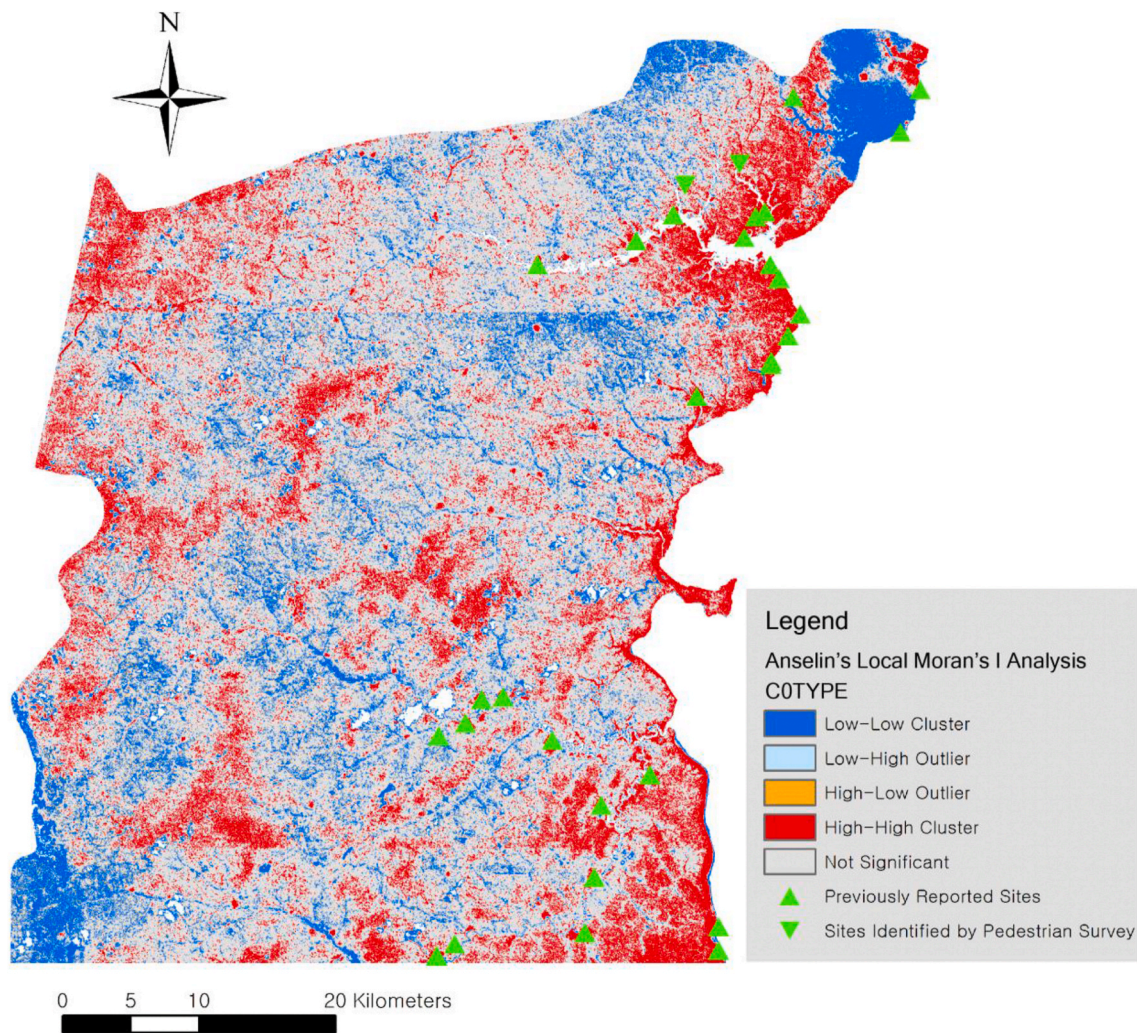


Fig. 7. The model created through Anselin's Local Moran's I of EVI values.

threshold distance that is appropriate for the research purpose (ESRI, 2016).

For our research objectives, we utilized a threshold distance set as a fixed distance of 80 m with the weighted values of the EVI as described above. This process has been achieved by selecting “FIXED\_DISTANCE\_METHOD” for the “Conceptualization of Spatial Relationships” option in the Getis-Ord’s  $G_i^*$  analysis and Anselin’s Local Moran’s I analysis in ArcGIS. The threshold distance was set according to the size of the majority of ADE sites from this region, which can be interpreted as focal points of pre-Columbian landscape domestication. For this region, 80% of the sites are not larger than 2 ha (Kern et al., 2003) which is encapsulated within an  $80 \times 80$  m area. Therefore, in order to balance precision with analytical efficiency in order to capture three pixels in each cardinal direction in the autocorrelation, we limited the range of analysis to 80 m.

### 2.5. Validation of the model

The models to predict the areas affected by pre-Columbian landscape domestication were validated using a combination of spatial-statistical and field techniques. The first method compared the distribution of EVI values between the ADE sites and the FNC. It utilized the location of the previously reported ADE sites in the FNC (Lisboa et al., 2013). The location of the ADE sites was loaded into the GIS. Then buffers with the radius of 80 m were generated around the location of the ADE sites, according to the postulated site size. A histogram of the  $G_i$  Bin and

COType, which are collected from the EVI points that are within the 80 m radius, was generated to represent the clustering pattern of EVI values of the ADE sites. To statistically gauge the potential range of variance for EVI distribution in the FNC, 2000 random points were generated in order to compare the population of known ADE sites against random permutations of points. Buffers of 80 m radius were generated for the random points as well.  $G_i$  Bin and COType from the EVI points within the 80 m radius were aggregated and used to create a histogram that displays the clustering pattern of EVI values of the FNC. The histograms of the  $G_i$  Bin and COType of each ADE site and the FNC were compared. Through this comparison, the effect of ADE sites on EVI was observed.

The other method involved undertaking a pedestrian archaeological survey and shovel tests according to the maps that visualize the created models. The points for pedestrian surveys were selected within the areas where ADE sites were not previously reported. For the pedestrian survey, the created map was loaded to a Garmin Montana 680t GPS device for navigation to the targeted location. Vegetation structure and composition were noted within the survey zones. Following the shovel tests, the solums were documented and sampled, and an Oakfield coring probe was used to constrain the sizes of the sites.

## 3. Results

### 3.1. Results of ANOVA using soil class and EVI

According to the summarized statistics of the EVI (Table 2),

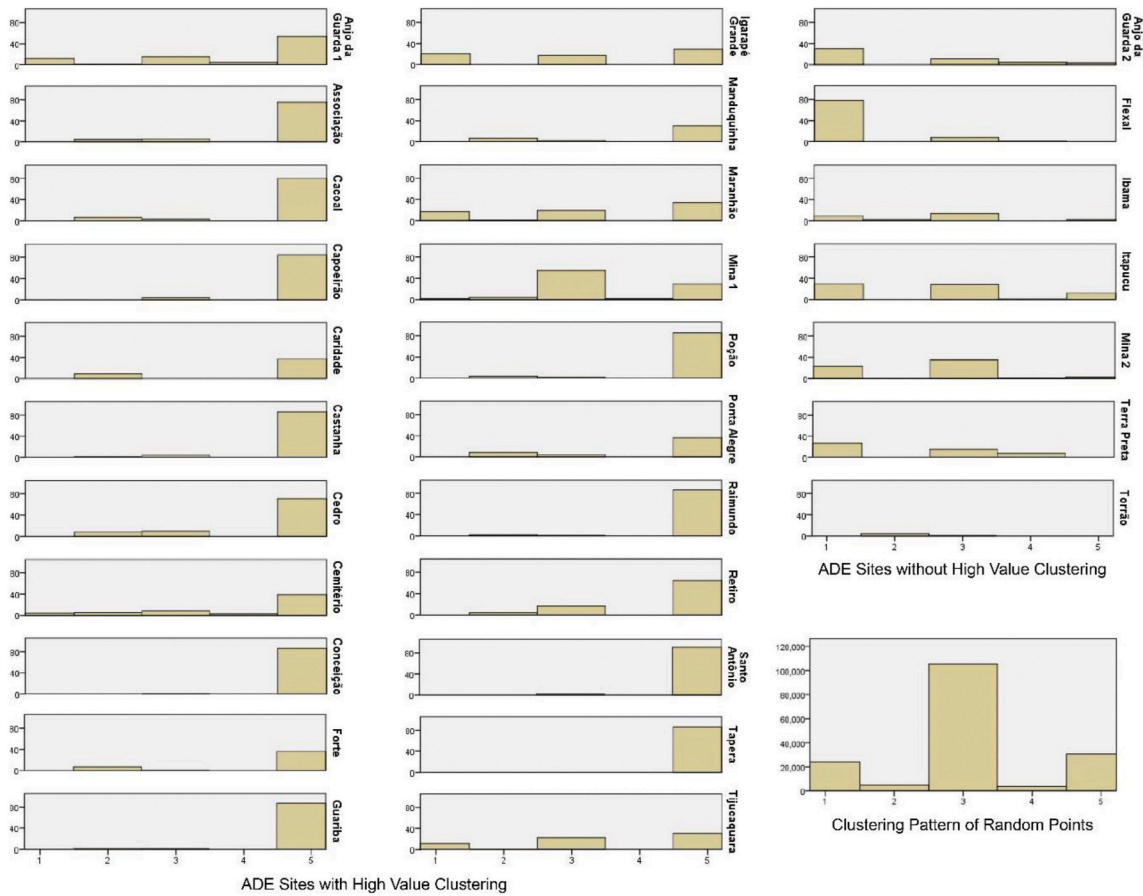


**Fig. 8.** The classification of the sites into ‘ADE Sites with High-Value Clustering’ and ‘ADE Sites without High-Value Clustering’ according to the model created by Anselin’s Local Moran’s I Analysis of EVI values. The numbers of the x-axis indicate the C0Type (1 = Low-Low Cluster, 2 = Low-High Outlier, 3 = Not Significant, 4 = High-Low Outlier, 5 = High-High Cluster). The classification was made by comparing the percentage of the points classified with the C0Type of High-High Cluster, indicated by the number 5. The y-axis indicates the number of points. If the sites consisted of a higher percentage of points with C0Type of High-High Cluster than 2000 randomly generated points that represent the FNC, they were classified as ‘ADE Sites with High Value Clustering.’ If not, they were classified as ‘ADE Sites without High Values Clustering.’

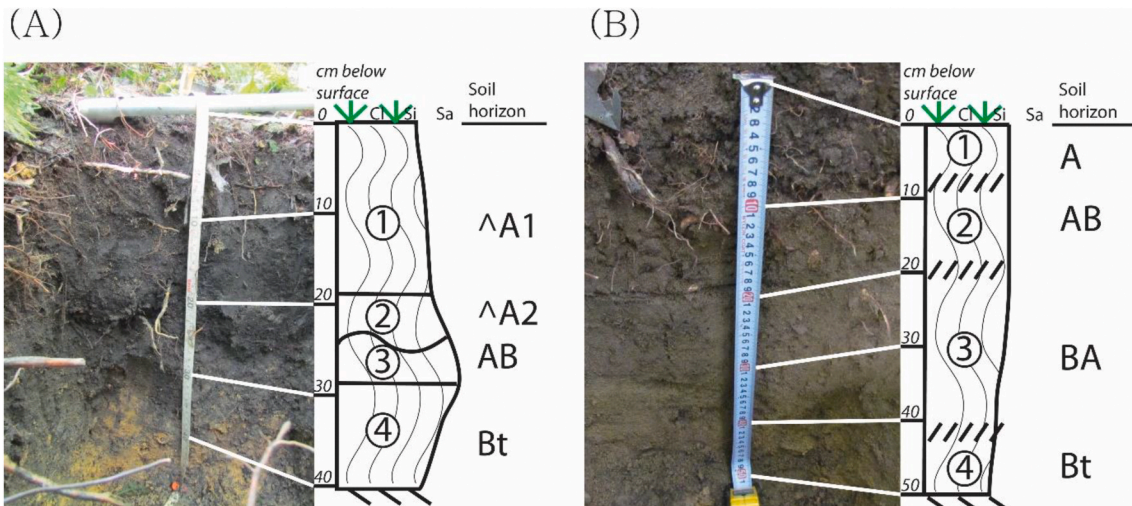


**Fig. 9.** Profiles of (A) CAX1 and (B) CAX3 sites, which were identified during the pedestrian survey.

distinguished by the base soil type mapped in [Costa et al. \(2005\)](#), it is evident that there is a difference in EVI values between different soil types. Even though the range of EVI values is limited since values smaller than 0.8753 were excluded, for explicit comparison between the

forest environment, it is clear that there is a difference in the EVI values between soil types when observing the upper and lower bounds of the 95% confidence interval from the mean value do not overlap between soil types with high EVI values, such as Plinthosol (FTbd), and soil types

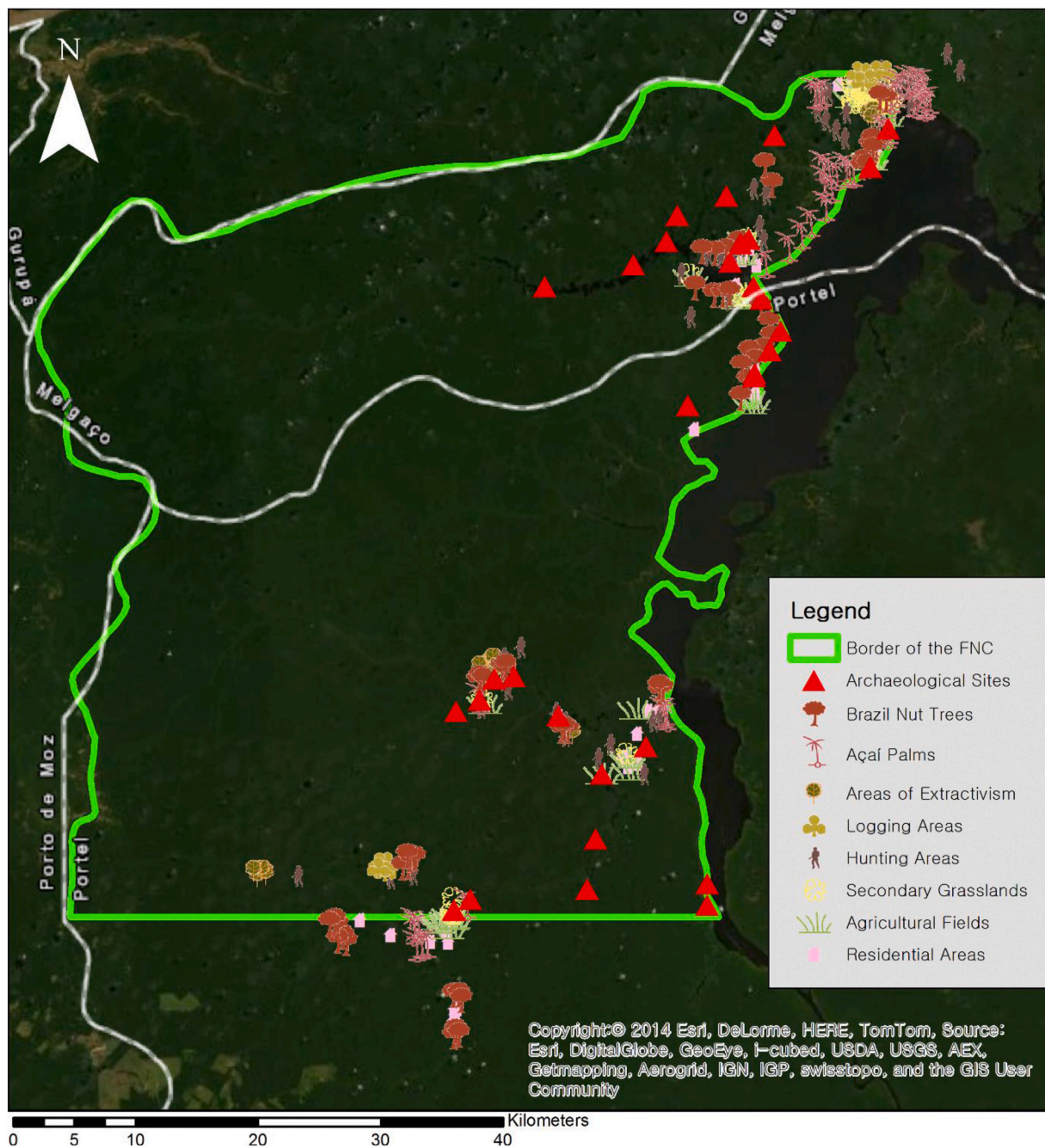


Fig. 10. Location of archaeological sites and modern human activity areas in the FNC.

with low EVI values, such as Latosol (LAd1). The summarized statistics indicate that EVI values do differ by soil types. The F-value result of the ANOVA test (Table 3) demonstrates that there is a statistically significant difference in the distribution of EVI values between the soil types such that the null hypothesis (there is a random relationship between soil class and EVI values) is rejected ( $p < 0.000$ ).

The result of Scheffe's post-hoc test compares the means of EVI values between different soil types in detail. The result demonstrates that the soil classes can be classified into six subsets by the mean of EVI values (Table 4). Soil classes LAd1, LAd4, and PAd1 have no significant difference with each other in mean EVI value (Cluster 1 in Fig. 4). The mean EVI value of soil classes FTbd and RUBd are not significantly different as well (Cluster 2 in Fig. 4). However, the rest of the soil classes can be distinguished from each other by statistically significant differences in the mean of EVI values (Fig. 4). The detailed result of the

Scheffe's post-hoc test is provided in the Supplementary Online Material 1.

### 3.2. The models and comparisons with previously reported sites

The EVI clustering pattern of the FNC is demonstrated by points within 80 m radius of the 2000 randomly generated points (see bottom right of Fig. 6 and 8). Based on the model created by the Getis-Ord's  $G_i^*$  (Fig. 5), 30% of the points around the 2000 points in the FNC test area had a  $G_i$  Bin value 3, which indicates high-value EVI cluster. Using this test threshold, we established the protocol that if more than 30% of the points within 80 m of an unknown point has the  $G_i$  Bin value 3, the site was classified as a high-probability ADE site with high-EVI value clustering. According to this classification scheme, 20 out of 29 previously documented archaeological sites were identified in zones of high EVI



Fig. 11. UAV photograph of the Ibama site showing modern land clearance. Photo credit: Bruno Moraes.

value clustering (Fig. 6).

According to the model generated by the Anselin's Local Moran's I (Fig. 7), approximately 13% of the points within 80 m radius of the 2000 randomly assigned points that represent the clustering pattern of the EVI values across the FNC were given the C0Type 'High-High Cluster', which indicates high EVI value clustering. Based on this criterion, and padding the results to reduce over-sampling noise, if the percentage of the points classified as points of 'High-High Cluster' within 80 m around archaeological sites was greater than 20%, the site was classified as a high-probability ADE site with high value clustering. According to this classification scheme, 22 out of 29 previously documented archaeological sites inside the FNC were identified in zones of high EVI values (Fig. 8).

Out of the sites included in the analysis, two previously identified archaeological sites (Mina 1 and Tijucaquera) were classified differently by the models created by Getis-Ord's  $G_i^*$  and Anselin's Local Moran's I. While Mina 1 and Tijucaquera sites were identified as ADE sites without high EVI value clustering by Getis-Ord's  $G_i^*$  analysis, they were classified as ADE sites with high EVI value clustering by Anselin's Local Moran's I analysis. Besides these two sites, the other 27 sites were classified the same by both spatial autocorrelation analysis of the EVI values.

### 3.3. Results of pedestrian surveys and soil profiling

Pedestrian surveys and soil profiling were carried out in July 2016. Soil profiles were documented at eight locations (Fig. 3), and a pedestrian survey was performed during the navigation to the points of soil profiles. The detailed soil profiles are provided in the Supplementary Online Material 2. The areas demonstrated various degrees of influence of landscape domestication.

The previously undocumented site identified in the spatial model that showed the strongest influence of landscape domestication was the site designated CAX1. The topsoil of CAX1 is a black (10YR2/1) sandy clay loam with a very weak sub-angular blocky structure and has no preserved bedding or depositional features (Fig. 9). CAX1 was classified as ADE with ceramic and charcoal inclusions identified in the profile, indicating human activity on site. There were no trails in and around CAX1, suggesting the site had been abandoned for some time. The forest

was covered with wood thickets, indicating that it is a secondary forest.

Another locale with evidence of landscape domestication was IBA4. IBA4 also had organically-enriched, black topsoil of ADE, but while CAX1 was an ADE site, IBA4 was located approximately 100 m from the core of the Ibama site, which has been previously reported (Lisboa et al., 2013). The color of the topsoil of IBA4 was lighter in hue (10YR3/1), nevertheless several anthropogenic tree species were documented, including mango (*Mangifera indica*) and rubber (*Hevea brasiliensis*) trees.

CAX3 is another locale that contained traits of an area influenced by landscape domestication. The topsoil was slightly darker than the natural rainforest soils, with the color of 10YR3/2 (strong brown). The topsoil was comprised of a sandy clay loam with a moderate sub-angular blocky structure and also lacks bedding or depositional structure (Fig. 9). CAX3 site lacks ceramics but has abundant charcoal inclusions in its profile.

IBA3 is located on the trail linking the Ibama site and the Forte site. Although the topsoil of IBA3 did not demonstrate characteristics of ADE the top layer of the soil was thickened. A remnant of a recently abandoned house and debris of modern human activity, such as plastic, were identified around the point. Also, trees that local people make use of were documented, such as Brazil nut (*Bertholletia excelsa*) and açai palms (*Euterpe oleracea*).

FOR1 is 95 m away from the Forte site. The A horizon of the topsoil was slightly darker than typical rainforest soils (10 YR 3/2). Although some plants that seemed to have been managed by humans, such as cacao (*Theobroma cacao*), were identified during pedestrian reconnaissance.

IBA5 was located on an upper terrace from the passage that links the Ibama site and the Forte site. The A horizon was slightly darker than typical rainforest soils (10 YR 3/3) but had general phenotypic characteristics of Ultisols. No plants were identified that were known to have been used by local people, however the density of the forest was relatively thick, which may indicate a secondary forest.

CAX2 was approximately 250 m away from CAX1. The soil was Ultisol, which is common in the tropical rainforest. No plants were identified that were known to have been used by local people. The forest in this area had the greatest density among the forests near all survey points.

IBA1 was a cutbank profile that has been exposed due to fluvial erosion. IBA1 consists mostly of a thick deposit of silty clay, which is approximately 5-m deep and is strongly cemented with strong redox-imporphic masses. The color of the topsoil is reddish, ranging from 5 YR 7/8 to 7.5 YR 5/3.

#### 4. Discussion

The ANOVA results demonstrate that the difference in soil characteristics is reflected in EVI. Since it has been shown that soil characteristics are affected by landscape domestication activities, the result of the ANOVA reflects the connection between the landscape domestication activities and the growth of secondary vegetation that can be identified in the EVI. The comparison between the clustering patterns of EVI values of the centers of landscape domestication, which are ADE sites, and the general clustering pattern of EVI values of the FNC proposed that landscape domestication enhances the EVI values. According to this result, to trace and calibrate landscape domestication in areas with minimal modern human disturbance such as FNC, researchers should focus on areas of high EVI value clusters. The widespread distribution of potential hotspots based on high EVI value clusters suggests persistent anthropic effects on vegetation from pre-Columbian through the present, regardless of the actual formation of ADE (see also Levis et al., 2017).

However, our results contrast Thayn et al. (2011) and Palace et al. (2017). Their results showed that ADE sites tend to have lower average EVI values. This contrasting result may have been caused by modern land use. According to Thayn et al. (2011), most of the ADE sites are currently used by local farmers, who recognize the productivity of these anthropic soils. This is also true in the case of the FNC as well. When comparing the location of modern human land use in the FNC (Fig. 10) and the location of ADE sites, ten out of 31 sites are located within 500 m of modern human activity areas. If modern human activities take place, which involves deforestation, such as agriculture or land clearance for residence, it will result in lower vegetation index values in the area (Morton et al., 2006).

It is difficult to demonstrate that modern human activities affected the results since the land use of small farmers in Amazonia shows great variability between households, based on conditions such as available labor and duration of stay (Marquette, 1998). Also, whether the small farmers of Amazonia clear the forest for timber and other purposes or preserve the forest for non-timber extraction is not established in a systematic manner, as modern industrialized farmers do (Summers et al., 2004; Junqueira et al., 2011). Therefore, the type of land use in a certain area can be changed into various forms within a relatively short period (Fearnside, 1996). For instance, a fully cleared agricultural field may be transformed into a woody secondary forest within three years (Fearnside, 1996).

The complexity of modern land use is reflected in the current research as well, and it is difficult to verify whether the modern land use affected the spatial model. However, at least one site clearly shows that the land clearance by modern human activity results in the absence of high EVI value clustering. The Ibama site has been not classified as having high EVI value clustering, and a research station has been in operation by IBAMA since 1993 (Fig. 11). The land has been cleared since the establishment of the research station and results in the low EVI value-clustering pattern of the Ibama site.

The relationship between modern land clearance by small farmers and VIs has not been fully explored in the FNC. However, it is evident that land clearance results in low VI values (Borini Alves et al., 2015; Morton et al., 2006), and considering the case of the Ibama site, modern land clearance may be the main cause of the presence of sites without high EVI value clustering in the FNC, though there may be exceptions. Therefore it can be said that ADE sites tend to provide high EVI value clustering patterns, when they are located in a forest environment that is not subject to heavy commercial logging or ranching (Querino et al.,

2016). In 2018, the size of the forested area in the Brazilian Amazon is approximately 2.9 million km<sup>2</sup> of the area that measures 5,068,048 km<sup>2</sup> monitored by PRODES (2020), which is a deforestation monitoring system developed by the *Instituto Nacional de Pesquisas Espaciais*. Protected areas, such as the FNC, are less subject to large-scale deforestation (Jusys, 2018), which we hypothesize as the main reason high VI values correlate to nutrient-rich anthrosols, such as ADEs.

The attributes related to the research material, spatial resolution of the satellite images and the size of the majority of the ADE sites, may be factors that are contributing to the contradicting results with Thayn et al. (2011) and Palace et al. (2017). The majority of the ADE sites are less than 2 ha in size (Kern et al., 2003). However, the resolution of the MODIS series, the satellite images that Thayn et al. (2011) and Palace et al. (2017) utilized, is 250 m per pixel (each pixel covers an area greater than 6 ha). The model presented in this research and the results of a pedestrian survey demonstrate that there are sites that cannot be detected with the 250 m/pixel resolution. For example, CAX1, which is an ADE site identified by the pedestrian survey, cannot be detected with 250 m/pixel resolution, since it is surrounded by low-value clustering EVI values. On the other hand, in river valleys and areas with sustained and ongoing forest resource management, oversampling of high-value EVI clusters limits the potential applicability of the tool for use to locate ADE sites. Therefore, the results of this pilot research suggest that the method developed here is most effective in identifying small (<6 ha) ADE sites located on *terra firme* away from large riverine settings based on contrasting, adjacent EVI cluster values, which are also those sites that are most difficult to locate on pedestrian survey.

The overall results presented indicate that EVI combined with spatial autocorrelation methods can be a useful tool in tracing and calibrating landscape domestication in Amazonia. However, the modern landscape represented in VIs is susceptible to modern human land use. Therefore, before identifying landscape domestication through VIs, a firm understanding of the effects of modern land use on VIs within a specific project area is required. It is also important to utilize satellite images with a spatial resolution that fits the research purpose.

#### 5. Conclusion

The results of the geospatial analyses conducted here offer an interpretation of the relationship between soils, landscape domestication, and EVI in the FNC that can be applied more generally to improve archaeological site detection in the Amazon and other tropical rainforest settings. This research is one of the few regional level studies that involve remote sensing in Amazonia, while a majority of the preceding research has set the scale of the research at a continental or sub-continental level, covering the entire Amazonia. The results provided in this paper are context-specific to the FNC, which cannot be uncritically applied to the general patterns of Amazonia. For example, different statistical sorting thresholds of EVI values should be established based on the amount of disturbance or cloud cover present in the satellite images. However, the method was designed to be replicated and tested in other settings, most especially in circumstances to anticipate archaeological surveys or conservation efforts aimed at preserving ADE. The satellite images used are free to the public and software is off-the-rack (though proprietary) and commonly available at research institutions.

Limiting the research area to the FNC is one of the most critical elements of this research. The heterogeneity of the natural and anthropic environment in Amazonia has been repeatedly demonstrated (McMichael et al., 2014; Shepard and Ramirez, 2011). Therefore, an attempt to understand the aspect or the scale of landscape domestication in Amazonia as a whole cannot be achieved by a single research project, but by accumulating several regional scales research projects of this nature. Also, the characteristics of the FNC as protected by the national government from commercial logging, mining, and ranching, has created a semi-controlled research area. However, this is not the case for most of

the other regions in Amazonia. Therefore, although the results that have been presented in this research may be further contextualized by future studies, it can provide a starting point for the studies that attempt to trace and calibrate landscape domestication in Amazonia on a regional scale. This also shows the importance of protected areas, not only for obvious conservation purposes, but also for long-term monitored monitored/controlled scientific research on climate, environment, etc.

While the application of the results of the research in other landscapes of Amazonia is needed, further research on the relationship between vegetation structure and other elements of landscapes should be explored for the application. Especially, more research is required on areas where modern human land use has significant impact in which archaeological sites and endangered habitats are more vulnerable to human destruction. Further understanding on the relationship between VIs and landscape would assist monitoring natural and archaeological resources of Amazonia.

### Declaration of competing interest

The authors declare that they have no known competing financial interests or personal relationships that could have appeared to influence the work reported in this paper.

### Acknowledgments

This research was supported by Korea-US International Cooperation through the National Research Foundation of Korea (NRF) funded by the Ministry of Science, ICT & Future Planning (NRF2015068576) (DKW), the CORE Program through the NRF funded by the Korean Ministry of Education (DKW), Wenner-Gren Foundation grant #9566 (DKW) and National Geographic Society grant #EC-KOR-223R-18 (JC). Permission to conduct field research was provided by the Polícia Federal Brasil and the Ministério da Ciência, Tecnológica e Inovação under the auspices of a research visa (015474 ML) granted to David K. Wright. Permission to conduct archaeological research was provided by the Instituto do Patrimônio Histórico e Artístico Nacional (#01492.000340/2015-01) and by the ICBio (# 5533230) to Helena Pinto Lima. We thank the support of Museu Paraense Emílio Goeldi in facilitating all aspects of the research. Specific thanks are given to Socorro Andrade, Director of Estação Científica Ferreira Penna in the Caxiuanã National Forest. Richard Pace and Andrew Wyatt of Middle Tennessee State University (MTSU) were crucial elements of success in this project for running the 2016 MTSU Archaeological Field School in Amazon, which provided a cohort of student workers and providing crucial logistical support. Local crew provided us outstanding guides and boats through the rainforest, with special thanks to “Mo.” We are also grateful to the College of Humanities of Seoul National University (SNU) for providing the laboratory facilities and ArcGIS site licenses for GIS analysis that provided the backbone of this research.

### Appendix A. Supplementary data

Supplementary data to this article can be found online at <https://doi.org/10.1016/j.jas.2020.105240>.

### References

- Anselin, L., 1995. Local indicators of spatial association—LISA. *Geogr. Anal.* 27, 93–115. <https://doi.org/10.1111/j.1538-4632.1995.tb00338.x>.
- Arroyo-Kalin, M., 2014. The variability of Amazonian Dark Earths: comparing anthropogenic soils from three regions of the Amazonian biome. In: Rostain, S. (Ed.), *Antas de Orellana - Actas del 3er Encuentro Internacional de Arqueología Amazónica*. Instituto Francés de Estudios Andinos, Quito, pp. 323–329.
- Arroyo-Kalin, M., Neves, E., Woods, W., 2009. Anthropogenic dark earths of the central Amazon region: remarks on their evolution and polygenetic composition. In: Woods, W.I., Teixeira, W.G., Lehmann, J., Steiner, C., WinklerPrins, A., Rebellato, L. (Eds.), *Amazonian Dark Earths: Wim Sombroek's Vision*. Springer Netherlands, Dordrecht, pp. 99–125. [https://doi.org/10.1007/978-1-4020-9031-8\\_5](https://doi.org/10.1007/978-1-4020-9031-8_5).
- Arvor, D., Jonathan, M., Meirelles, M.S.P., Dubreuil, V., Durieux, L., 2011. Classification of MODIS EVI time series for crop mapping in the state of Mato Grosso, Brazil. *Int. J. Rem. Sens.* 32, 7847–7871. <https://doi.org/10.1080/01431161.2010.531783>.
- Balée, W., 1998. *Historical ecology: premises and postulates*. In: Balée, W. (Ed.), *Advances in Historical Ecology*. Columbia University Press, New York, pp. 13–29.
- Balée, W.L.E., Clark, L., 2006. *Time and Complexity in Historical Ecology: Studies in the Neotropical Lowlands*. Columbia University Press, New York.
- Behling, H., da Costa, M.L., 2000. Holocene environmental changes from the Rio Curuá record in the Caxiuanã region, eastern Amazon basin. *Quat. Res.* 53, 369–377. <https://doi.org/10.1006/qres.1999.2117>.
- Birk, J.J., Teixeira, W.G., Neves, E.G., Glaser, B., 2011. Faeces deposition on amazonian anthrosols as assessed from 5 $\beta$ -stanols. *J. Archaeol. Sci.* 38, 1209–1220. <https://doi.org/10.1016/j.jas.2010.12.015>.
- Borini Alves, D., Pérez-Cabello, F., Mimbreno, M.R., 2015. Land-use and land-cover dynamics monitored by NDVI multitemporal analysis in a selected southern Amazonian area (Brazil) for the last three decades. In: Schreier, G., Skrovseth, P.E., Staudenrausch, H. (Eds.), *The International Archives of the Photogrammetry, Remote Sensing and Spatial Information Sciences, Volume XL-7/W3*, 36<sup>th</sup> International Symposium on Remote Sensing Environment, Berlin, Germany, 11–15 May 2015, pp. 329–335. <https://doi.org/10.5194/isprsarchives-XL-7-W3-329-2015>.
- Browne Ribeiro, A.T., 2014. Houses, hearths, and gardens: space and temporality in a pre-Columbian village in the Central Amazon. In: Rostain, S. (Ed.), *Antas de Orellana - Actas del 3er Encuentro Internacional de Arqueología Amazónica*. Instituto Francés de Estudios Andinos, Quito, pp. 183–189.
- Bush, M.B., Silman, M.R., 2007. Amazonian exploitation revisited: ecological asymmetry and the policy pendulum. *Front. Ecol. Environ.* 5, 457–465. <https://doi.org/10.1890/070018>.
- Bush, M.B., Silman, M.R., McMichael, C., Saatchi, S., 2008. Fire, climate change and biodiversity in Amazonia: a late-Holocene perspective. *Phil. Trans. R. Soc. B.* 363, 1795–1802. <https://doi.org/10.1098/rstb.2007.0014>.
- Clement, C.R., Denevan, W.M., Heckenberger, M.J., Junqueira, A.B., Neves, E.G., Teixeira, W.G., Woods, W.I., 2015. The domestication of Amazonia before European conquest. *Proc. R. Soc. B* 282, 20150813. <https://doi.org/10.1098/rspb.2015.0813>.
- Coirolo, A.D., d'Aquino, G.I.d.R., 2005. *Salvamento Arqueológico no Sítio Ilha de Terra, Região de Caxiuanã, Melgaço, Pará, Congresso da Sociedade de Arqueologia Brasileira. Sociedade de Arqueologia Brasileira, Campo Grande*.
- Coluzzi, R., Lanorte, A., Lasaponara, R., 2010. On the LiDAR contribution for landscape archaeology and palaeoenvironmental studies: the case study of Bosco dell'Incoronata (Southern Italy). *Adv. Geosci.* 24, 125–132. <https://doi.org/10.5194/adgeo-24-125-2010>.
- Costa, F.d.A., 2003. *A Cerâmica do Sítio Arqueológico Ilha de Terra - Caxiuanã (PA). Museu Paraense Emílio Goeldi, Belém*.
- Costa, J.A., Lima da Costa, M., Kern, D.C., 2013. Analysis of the spatial distribution of geochemical signatures for the identification of prehistoric settlement patterns in ADE and TMA sites in the lower Amazon Basin. *J. Archaeol. Sci.* 40, 2771–2782. <https://doi.org/10.1016/j.jas.2012.12.027>.
- Costa, J.A., Rodrigues, T.E., Kern, D.C., 2009. Os solos da Estação Científica Ferreira Penna, Caxiuanã. In: Lisboa, P.L.B. (Ed.), *Caxiuanã: Desafios para a conservação de uma Floresta Nacional na Amazônia*. Museu Paraense Emílio Goeldi, Belém, pp. 117–127.
- Costa, J.A., Rodrigues, T.E., Kern, D.C., Silva, J.M.d.L.e., 2005. Classificação e distribuição dos padrões pedogeomórficos da Estação Científica Ferreira Penna, na região de Caxiuanã, no estado do Pará. *Bol. Mus. Para. Emílio Goeldi, sér. Ciências Naturais* 1, 117–128. <http://repositorio.museu-goeldi.br:8080/jspui/handle/mgoeldi/514>.
- Erickson, C.L., 2008. Amazonia: the historical ecology of a domesticated landscape. In: Silverman, H., Isbell, W.H. (Eds.), *The Handbook of South American Archaeology*. Springer New York, New York, pp. 157–183. [https://doi.org/10.1007/978-0-387-74907-5\\_11](https://doi.org/10.1007/978-0-387-74907-5_11).
- ESRI, 2016. ArcGIS Pro Tool Reference. <http://pro.arcgis.com/en/pro-app/tool-reference/spatial-statistics>. (Accessed 13 December 2019).
- Evans, C., Meggers, B.J., 1950. Preliminary results of archaeological investigations at the mouth of the Amazon. *Am. Antiq.* 16, 1–9. <https://doi.org/10.2307/276335>.
- Fearnside, P.M., 1996. Amazonian deforestation and global warming: carbon stocks in vegetation replacing Brazil's Amazon forest. *For. Ecol. Manag.* 80, 21–34. [https://doi.org/10.1016/0378-1127\(95\)03647-4](https://doi.org/10.1016/0378-1127(95)03647-4).
- Fraser, J., Teixeira, W., Falcão, N., Woods, W., Lehmann, J., Junqueira, A.B., 2011. Anthropogenic soils in the Central Amazon: from categories to a continuum. *Area* 43, 264–273. <https://doi.org/10.1111/j.1475-4762.2011.00999.x>.
- Gandhi, G.M., Parthiban, S., Thummalu, N., Christy, A., 2015. NDVI: vegetation change detection using remote sensing and GIS – a case study of Vellore district. *Procedia Comput. Sci.* 57, 1199–1210. <https://doi.org/10.1016/j.procs.2015.07.415>.
- Getis, A., Ord, J.K., 1992. The analysis of spatial association by use of distance statistics. *Geogr. Anal.* 24, 189–206. <https://doi.org/10.1111/j.1538-4632.1992.tb00261.x>.
- Hecht, S.B., 2003. Indigenous soil management and the creation of Amazonian Dark Earths: implications of Kayapó practice. In: Lehmann, J., Kern, D.C., Glaser, B., Woods, W.I. (Eds.), *Amazonian Dark Earths: Origin Properties Management*. Springer Netherlands, Dordrecht, pp. 355–372. [https://doi.org/10.1007/1-4020-2597-1\\_18](https://doi.org/10.1007/1-4020-2597-1_18).
- Huete, A., Didan, K., Miura, T., Rodriguez, E.P., Gao, X., Ferreira, L.G., 2002. Overview of the radiometric and biophysical performance of the MODIS vegetation indices. *Remote Sens. Environ.* 83, 195–213. [https://doi.org/10.1016/S0034-4257\(02\)00096-2](https://doi.org/10.1016/S0034-4257(02)00096-2).
- Jiang, Z., Huete, A.R., Didan, K., Miura, T., 2008. Development of a two-band enhanced vegetation index without a blue band. *Remote Sens. Environ.* 112, 3833–3845. <https://doi.org/10.1016/j.rse.2008.06.006>.

- Junqueira, A.B., Shepard, G.H., Clement, C.R., 2011. Secondary forests on anthropogenic soils of the middle Madeira river: valuation, local knowledge, and landscape domestication in Brazilian Amazonia. *Econ. Bot.* 65, 85–99. <https://doi.org/10.1007/s12231-010-9138-8>.
- Jusys, T., 2018. Changing patterns in deforestation avoidance by different protection types in the Brazilian Amazon. *PLoS One* 13, e0195900. <https://doi.org/10.1371/journal.pone.0195900>.
- Kern, D.C., 2004. *Processos de Formação de Solos com Terra Preta Arqueológica na Amazônia*. Museu Paraense Emílio Goeldi, Belém.
- Kern, D.C., d' Aquino, G., Rodrigues, T.E., Frazao, F.J.L., Sombroek, W., Myers, T.P., Neves, E.G., 2003. Distribution of amazonian dark earths in the Brazilian Amazon. In: Lehmann, J., Kern, D.C., Glaser, B., Woods, W.I. (Eds.), *Amazonian Dark Earths: Origin Properties Management*. Springer Netherlands, Dordrecht, pp. 51–75. [https://doi.org/10.1007/1-4020-2597-1\\_4](https://doi.org/10.1007/1-4020-2597-1_4).
- Kim, H., 2012. Analysis of change in the population distribution based on spatial relationship using the Sphere of Influence. *The Korea Spat. Plann. Rev.* 73, 47–61 (in Korean). <http://www.riss.kr/link?id=A101618726>.
- Lehmann, J., Pereira da Silva, J., Steiner, C., Nehls, T., Zech, W., Glaser, B., 2003. Nutrient availability and leaching in an archaeological Anthrosol and a Ferralsol of the Central Amazon basin: fertilizer, manure and charcoal amendments. *Plant Soil* 249, 343–357. <https://doi.org/10.1023/a:1022833116184>.
- Levis, C., Costa, F.R.C., Bongers, F., Peña-Claros, M., Clement, C.R., Junqueira, A.B., Neves, E.G., Tamanaha, E.K., Figueiredo, F.O.G., Salomão, R.P., Castilho, C.V., Magnusson, W.E., Phillips, O.L., Guevara, J.E., Sabatier, D., Molino, J.-F., López, D. C., Mendoza, A.M., Pitman, N.C.A., Duque, A., Vargas, P.N., Zartman, C.E., Vasquez, R., Andrade, A., Camargo, J.L., Feldpausch, T.R., Laurance, S.G.W., Laurance, W.F., Killeen, T.J., Nascimento, H.E.M., Montero, J.C., Mostacedo, B., Amaral, I.L., Guimarães Vieira, I.C., Brienen, R., Castellanos, H., Terborgh, J., Carim, M.d.J.V., Guimarães, J.R.d.S., Coelho, L.d.S., Matos, F.D.d.A., Wittmann, F., Mogollón, H.F., Damasco, G., Dávila, N., García-Villacorta, R., Coronado, E.N.H., Emilio, T., Filho, D.d.A.L., Schiatti, J., Souza, P., Targhetta, N., Comiskey, J.A., Marimon, B.S., Marimon, B.-H., Neill, D., Alonso, A., Arroyo, L., Carvalho, F.A., de Souza, F.C., Dallmeier, F., Pansonato, M.P., Duivenvoorden, J.F., Fine, P.V.A., Stevenson, P.R., Araujo-Murakami, A., Aymard, C. G.A., Baraloto, C., do Amaral, D. D., Engel, J., Henkel, T.W., Maas, P., Petronelli, P., Revilla, J.D.C., Stropp, J., Daly, D., Gribel, R., Paredes, M.R., Silveira, M., Thomas-Caesar, R., Baker, T.R., da Silva, N.F., Ferreira, L.V., Peres, C.A., Silman, M.R., Cerón, C., Valverde, F.C., Di Fiore, A., Jimenez, E.M., Mora, M.C.P., Toledo, M., Barbosa, E.M., Bonates, L.C.d.M., Arboleda, N.C., Farias, E.d.S., Fuentes, A., Guillaumet, J.-L., Jørgensen, P.M., Malhi, Y., de Andrade Miranda, I.P., Phillips, J.F., Prieto, A., Rudas, A., Ruschel, A. R., Silva, N., von Hildebrand, P., Vos, V.A., Zent, E.L., Zent, S., Cintra, B.B.L., Nascimento, M.T., Oliveira, A.A., Ramirez-Angulo, H., Ramos, J.F., Rivas, G., Schöngart, J., Sierra, R., Tirado, M., van der Heijden, G., Torre, E.V., Wang, O., Young, K.R., Baider, C., Cano, A., Farfan-Rios, W., Ferreira, C., Hoffman, B., Mendoza, C., Mesones, I., Torres-Lezama, A., Medina, M.N.U., van Andel, T.R., Villarroel, D., Zagt, R., Alexiades, M.N., Balslev, H., Garcia-Cabrera, K., Gonzales, T., Hernandez, L., Huamantupa-Chuquimaco, I., Manzatto, A.G., Milliken, W., Cuenca, W.P., Pansini, S., Pauletto, D., Azevalo, F.R., Reis, N.F.C., Sampaio, A.F., Giraldo, L.E.U., Sandoval, E.H.V., Gamarra, L.V., Vela, C.I.A., ter Steege, H., 2017. Persistent effects of pre-Columbian plant domestication on Amazonian forest composition. *Science* 355, 925–931. <https://doi.org/10.1126/science.aal0157>.
- Levis, C., Flores, B.M., Moreira, P.A., Luize, B.G., Alves, R.P., Franco-Moraes, J., Lins, J., Konings, E., Peña-Claros, M., Bongers, F., Costa, F.R.C., Clement, C.R., 2018. How people domesticated Amazonian forests. *Front. Ecol. Evol.* 5 <https://doi.org/10.3389/fevo.2017.00171>.
- Lins, J., Lima, H.P., Baccaro, F.B., Kinupp, V.F., Shepard Jr., G.H., Clement, C.R., 2015. Pre-Columbian floristic legacies in modern homegardens of central Amazonia. *PLoS One* 10, e0127067. <https://doi.org/10.1371/journal.pone.0127067>.
- Lisboa, P.L.B., Bezerra, M.d.G.F., Cardoso, A.L.d.R., 2013. *Caxiuanã: História Natural e Ecologia de uma Floresta Nacional da Amazônia*. Museu Paraense Emílio Goeldi, Belém.
- Ma, B.L., Dwyer, L.M., Costa, C., Cober, E.R., Morrison, M.J., 2001. Early prediction of soybean yield from canopy reflectance measurements. *Agron. J.* 93, 1227–1234. <https://doi.org/10.2134/agronj2001.1227>.
- Macedo, R.S., Teixeira, W.G., Corrêa, M.M., Martins, G.C., Vidal-Torrado, P., 2017. Pedogenetic processes in anthrosols with prehistoric horizon (amazonian dark Earth) in central Amazon, Brazil. *PLoS One* 12, e0178038. <https://doi.org/10.1371/journal.pone.0178038>.
- Marquette, C.M., 1998. Land use patterns among small farmer settlers in the northeastern Ecuadorian Amazon. *Hum. Ecol.* 26, 573–598. <https://doi.org/10.1023/a:1018797325069>.
- McMichael, C.H., Correa-Metrio, A., Bush, M.B., 2012. Pre-Columbian fire regimes in lowland tropical rainforests of southeastern Peru. *Palaeogeogr. Palaeoclimatol. Palaeoecol.* 342–343, 73–83. <https://doi.org/10.1016/j.palaeo.2012.05.004>.
- McMichael, C.H., Palace, M.W., Bush, M., Braswell, B., Hagen, S., Neves, E., Silman, M., Tamanaha, E., Czarnecki, C., 2014. Predicting pre-Columbian anthropogenic soils in Amazonia. *Proc. R. Soc. B.* 281, 20132475. <https://doi.org/10.1098/rspb.2013.2475>.
- Meggors, B.J., 1971. *Amazonia: Man and Culture in a Counterfeit Paradise*. Chicago, Aldine, Atherton, Chicago.
- Morton, D.C., DeFries, R.S., Shimabukuro, Y.E., Anderson, L.O., Arai, E., del Bon Espiritito-Santo, F., Freitas, R., Morissette, J., 2006. Cropland expansion changes deforestation dynamics in the southern Brazilian Amazon. *Proc. Natl. Acad. Sci. U.S.A.* 103, 14637–14641. <https://doi.org/10.1073/pnas.0606377103>.
- Ord, J.K., Getis, A., 1995. Local spatial autocorrelation statistics: distributional issues and an application. *Geogr. Anal.* 27, 286–306. <https://doi.org/10.1111/j.1538-4632.1995.tb00912.x>.
- Palace, M.W., McMichael, C., Braswell, B.H., Hagen, S.C., Bush, M.B., Neves, E., Tamanaha, E., Herrick, C., Frolking, S., 2017. Ancient Amazonian populations left lasting impacts on forest structure. *Ecosphere* 8, e02035. <https://doi.org/10.1002/ecs2.2035>.
- Pandit, J.J., 2010. The analysis of variance in anaesthetic research: statistics, biography and history. *Anaesthesia* 65, 1212–1220. <https://doi.org/10.1111/j.1365-2044.2010.06542.x>.
- Pinter, N., Fiedel, S., Keeley, J.E., 2011. Fire and vegetation shifts in the Americas at the vanguard of Paleoindian migration. *Quat. Sci. Rev.* 30, 269–272. <https://doi.org/10.1016/j.quascirev.2010.12.010>.
- PRODES, 2020. Desmatamento nos Municípios da Amazônia Legal para o ano de 2018. <http://www.dpi.inpe.br/prdesdigital/prodesmunicipal.php>. (Accessed 20 January 2020).
- Querino, C.A.S., Beneditti, C.A., Machado, N.G., da Silva, M.J.G., Querino, J.K.A.d.S., Neto, L.A.d.S., Biudes, M.S., 2016. Spatiotemporal NDMI, LAI, albedo, and surface temperature dynamics in the southwest of the Brazilian Amazon forest. *J. Appl. Remote Sens.* 10, 026007 <https://doi.org/10.1117/1.JRS.10.026007>.
- Russell, J.C., 2005. *Integrated Approach to Predictive Modeling: A Case Study from the Upper Xingu (Mato Grosso, Brazil)*. PhD Thesis. University of Florida, Gainesville.
- Santos, H.d., Jacomine, P.K.T., Anjos, L.d., Oliveira, V.d., Oliveira, J.d., Coelho, M.R., Lumbrales, J.F., Cunha, T.d., 2006. *Sistema Brasileiro de Classificação de Solos, 2a edição ed. Embrapa, Brasília*.
- Santos, M.J., Disney, M., Chave, J., 2018. Detecting human presence and influence on neotropical forests with remote sensing. *Rem. Sens.* 10, 1593. <https://doi.org/10.3390/rs10101593>.
- Schmidt, M.J., Py-Daniel, A.R., de Paula Moraes, C., Valle, R.B., Caromano, C.F., Teixeira, W.G., Barbosa, C.A., Fonseca, J.A., Magalhães, M.P., do Carmo Santos, D.S., 2014. Dark earths and the human built landscape in Amazonia: a widespread pattern of anthrosol formation. *J. Archaeol. Sci.* 42, 152–165. <https://doi.org/10.1016/j.jas.2013.11.002>.
- Shepard, G.H., Ramirez, H., 2011. Made in Brazil: human dispersal of the Brazil nut (*bertholletia excelsa*, lecythidaceae) in ancient Amazonia. *Econ. Bot.* 65, 44–65. <https://doi.org/10.1007/s12231-011-9151-6>.
- Smith, N.J., 1980. Anthrosols and human carrying capacity in Amazonia. *Ann. Assoc. Am. Geogr.* 70, 553–566. <https://doi.org/10.1111/j.1467-8306.1980.tb01332.x>.
- Sombroek, W., 1966. *Amazon Soils: A Reconnaissance of the Soils of the Brazilian Amazon Region*. Center for Agricultural Publications and Documentation, PhD Thesis, Wageningen University, Wageningen.
- Summers, P.M., Browder, J.O., Pedlowski, M.A., 2004. Tropical forest management and silvicultural practices by small farmers in the Brazilian Amazon: recent farm-level evidence from Rondônia. *For. Ecol. Manag.* 192, 161–177. <https://doi.org/10.1016/j.foreco.2003.12.016>.
- Thayn, J., Price, K., Woods, W., 2009. Locating Amazonian Dark Earths (ADE) using satellite remote sensing – a possible approach. In: Woods, W.I., Teixeira, W.G., Lehmann, J., Steiner, C., WinklerPrins, A., Rebellato, L. (Eds.), *Amazonian Dark Earths: Wim Sombroek's Vision*. Springer Netherlands, Dordrecht, pp. 279–298. [https://doi.org/10.1007/978-1-4020-9031-8\\_14](https://doi.org/10.1007/978-1-4020-9031-8_14).
- Thayn, J.B., Price, K.P., Woods, W.I., 2011. Locating Amazonian Dark Earths (ADE) using vegetation vigour as a surrogate for soil type. *Int. J. Rem. Sens.* 32, 6713–6729. <https://doi.org/10.1080/01431161.2010.512941>.
- Walsh, S.J., Crawford, T.W., Welsh, W.F., Crews-Meyer, K.A., 2001. A multiscale analysis of LULC and NDMI variation in Nang Rong district, northeast Thailand. *Agric. Ecosyst. Environ.* 85, 47–64. [https://doi.org/10.1016/S0167-8809\(01\)00202-X](https://doi.org/10.1016/S0167-8809(01)00202-X).
- WinklerPrins, A., 2009. Sweep and char and the creation of amazonian dark earths in homegardens. In: Woods, W.I., Teixeira, W.G., Lehmann, J., Steiner, C., WinklerPrins, A., Rebellato, L. (Eds.), *Amazonian Dark Earths: Wim Sombroek's Vision*. Springer Netherlands, Dordrecht, pp. 205–211. [https://doi.org/10.1007/978-1-4020-9031-8\\_10](https://doi.org/10.1007/978-1-4020-9031-8_10).
- Yamamoto, H., Moriyama, M., Tsuchida, S., 2010. An assessment of atmospherically-corrected ASTER EVI from GEO grid. In: Kajiwar, K., Muramatsu, K., Soyama, N., Endo, T., Ono, A., Akatsuka, S. (Eds.), *International Archives of the Photogrammetry, Remote Sensing and Spatial Information Science, Volume XXXVIII, ISPRS Commission VIII Mid-term Symposium 'Networking the World with Remote Sensing'*, Kyoto, Japan, 9–12 August 2010, pp. 878–882. In: [https://www.isprs.org/proceedings/XXXVIII/part8/pdf/W08L73\\_20100308235930.pdf](https://www.isprs.org/proceedings/XXXVIII/part8/pdf/W08L73_20100308235930.pdf).